Western Mediterranean coastal plains show low resilience to the ongoing climate change

Abstract

Global sea level rise (GSLR) represents one of the most evident impacts of climate change. GSLR is expected to trigger widespread environmental changes, such as major coastal erosion and progressive inundation of large portions of low-elevated coastal zones. Such impacts will be particularly important in the large alluvial coastal plains which are considered the most vulnerable to the future GSLR. However, is it possible to define a common response for this type of coastal environment to climate change? Furthermore, what are the drivers that mostly control their evolution? We evaluated the potential resilience of 6 major western Mediterranean coastal plains to the future relative sea level rise, by examining the past response of the shoreline to modified sea-level rise rates. In each coastal plain, we statistically reconstructed the past variability in the sea-level rising rates analysing the geomorphic response (e.g., retreat, stability, or progradation) of the coastline to these changes. We then compared these data with the local RSLR (relative sea level rise) rates expected for the next decades (up to the year 2100) calculated considering different IPCC scenarios (i.e., SSP2-4.5, SSP3-7, SSP5-8.5) corrected for the coastal subsidence trends calculated in each coastal plain. This allowed us to predict the potential morphodynamic response of each plain to future sea level rise. Results indicate that only under the SSP2-4.5 scenario, we observe a minimal probability (e.g., < 13%) of natural resilience (equilibrium of the coastline). Under all the other scenarios, the investigated coastal plains are destined for an irreversible retreat trend.

Keywords: Sea level rise; coastal retreat; IPCC scenarios; coastal sensitivity, Mediterranean Sea

1. Introduction

In the second half of the 20th century, the Mediterranean population has doubled from 240 million to 480 million (UNEP, 2016; Cramer et al., 2018) and the human pressure on the coasts is further amplified by the increased international tourism. The Mediterranean coastal zone is thus characterized by an increased pressure from human activities, but also subject to future global environmental change. In fact, the Mediterranean area is considered a hotspot of current climate change (Guiot and Cramer, 2016; Cramer et al., 2018, Sarkar et al., 2022) where future warming is expected to exceed global rates by ~25% (Lionello and Scarascia, 2018). This may result in high sea-level rise rates compared to global averages, leading to significant losses in environmental, cultural and economic values of its coasts (Vacchi et al., 2021).

At the regional scale, the sea-level rise may be different from what is observed and modelled in open-ocean due to several factors, which also include natural vertical ground movements (VGMs) related to volcanic and/or tectonic activity, glacio-hydro-isostatic adjustment (GIA) and natural compaction of sediments (Mattei et al., 2022; Aucelli et al., 2021; Nicholls et al., 2021). VGMs are often enhanced by anthropic activities mainly related to groundwater overexploitation, gas extraction, and coastal over-settlement that can cause sea level variations higher than those expected at the global and regional scale. Furthermore, ocean dynamic factors (e.g., differences in the rates of oceanic thermal expansion, changes in long-term wind and atmospheric pressure) may cause large regional departures of up to 50%–100% from the global average change for the thermal expansion component of sea-level change (Nicholls et al., 2021).

There is an increasing availability of Mediterranean coastal inundation scenarios, notably for those sites which are particularly prone to the coupled effects of sea-level rise and negative vertical land motions such as the deltas and the coastal plains (e.g., Snoussi et al., 2008; Aucelli et al., 2017; Antonioli et al., 2017; Lopez-Doriga and Jimenez, 2020). These studies followed a variety of methodologies which are mainly based on the IPCC scenarios (corrected for the local GIA contribution) coupled with the assessment of local subsidence which can be derived from Holocene data (e.g. millennial-scale), from long tidal gauges (e.g., centennial-scale), GPS or InSAR data (e.g., decadal-scale). Most of the Mediterranean sea-level scenarios were based on a classical "bathtub" approach in which areas below the expected sea-level elevation are delineated as being flooded (e.g., Di Paola et al., 2021, Vandelli et al., 2022). This methodology is considered suitable for urban, armoured, rocky, and passive coasts characterized by moderate wave action and reduced sediment supply. However, "bathtub" inundation scenarios may be less accurate for active sedimentary coasts where future sea-level rise has more dynamic effects than inundation alone (Fitzgerald et al., 2008; Lopez-Doriga and Jimenez, 2020). In this morphological context, a wide range of processes driving coastal evolution are expected to occur which may counteract the incoming sea-level rise. However, the dynamic responses of shorelines and coastal environments (e.g., dune systems) are presently seldom taken into account in assessing the Mediterranean future scenarios to SLR.

The Mediterranean coasts were characterized by a continuous sea-level rise for the whole Holocene period (e.g., last 12 ka BP) with rates up to 10-15 mm a^{-1} followed by a major deceleration at 7 ka with rates lower than 3 mm a^{-1} (Vacchi et al., 2021). Since that period, the evolution of the Mediterranean coasts has been very different. Geological studies indicated that some coastal areas were affected by continuous erosion while others showed evidence of major progradation rates despite the continuous sea-level rise (i.e. Anthony et al., 2014; Melis et al., 2017; Degeai et al., 2020).

Such different response of coastal systems to sea level rise is controlled by the complex interplay of geomorphological (e.g., morphology of the coastal sector) and climatic factors which triggered modifications in fluvial activity and consequent increase/decrease of the solid transport (Anthony et al., 2014). The Holocene progradation trends of Mediterranean coastal plains show lots of variability as a consequence of local vertical movements (e.g., subsidence or uplift, that can amplify or reduce the effect of climatic sea-level rise) as well as in terms of sediment supply provided by the main rivers that play a fundamental role in the coastal adaptation to sea level rise (e.g., Voett et al., 2007; Anathony et al., 2014; Melis et al., 2017).

For these reasons, the past geomorphological response to the SLR, can be considered as a key-factor for the definition and validation of future inundation scenarios due to expected sea-level rise.

To this aim, in this study, we evaluated the response of 6 major Mediterranean coastal plains to the Holocene variability of sea-level rise. In particular, we used geological data to statistically quantify the thresholds of sea-level rising rates necessary to shift from a progradation to an erosive trend. These thresholds were used to infer the future response of the Mediterranean coastal plains to the different sea-level scenarios recently released by the Intergovernmental Panel of Climate Change (IPCC, 2023).

2. Methodology

We evaluated the potential coastal resilience of 6 major coastal plains located in the central and western Mediterranean Sea (Figure 1). These are the Valencia plain (Spain), Rhone plain (France), Arno, Tiber, Volturno and Sele plains (Italy).

We developed a specific coastal sensitivity index which integrates the past (e.g., last millennia) and recent (e.g., last decades) coastal evolution trends in order to evaluate the future evolution of the coastal plains on the basis of the expected sea level projections (IPCC, 2023).

We selected coastal plains widely investigated in the past. This allowed us to have a significant amount of information on the stratigraphic architecture and the past sea-level position thanks to the presence of a large number (e.g., 130) of Sea-Level Index Points (Shennan et al., 2015)

To define the **millennial trends**, we used radiocarbon-dated relict shorelines to constrain the precise timing of maximal mid-Holocene transgression. These data allowed us to define for each plain a phase of coastal retreat (i.e.,., the phase of a landward shift of the shoreline before the maximal mid-Holocene transgression), a phase of coastal equilibrium (i.e., a phase following the maximal transgression and characterised by very minor changes in depositional facies) and a phase of progradation (i.e., characterised by a major seaward shift of the shoreline caused by the global deceleration of the sea-level rising rates and the increased river inputs, Anthony et al., 2014; Melis et al., 2017; Ghilardi et al., 2017)

These morpho-evolutive data were coupled with the quantitative reconstruction of the millennial sea-level change rates by employing an Errors in Variables Integrated Gaussian Process model (EIV IGP, Cahill et al., 2015) on the suite Sea Level Index Points (SLIPs) available for each investigated coastal plain (Vacchi et al., 2016; 2021; Mattei and Vacchi, 2023).

This allowed us to obtain the **Millennial Trends Index** (MTI) which defines the past thresholds of sea-level rising rates to shift from i) coastal retreat, to ii) coastal equilibrium and iii) coastal progradation.

This allowed us to obtain the **Millennial Trends Index** (MTI) that defines the past thresholds of sea-level rising rates for each of the proposed phases (i.e., coastal retreat, coastal equilibrium, and coastal progradation).

To define the **recent morpho-evolutive trend,** we calculated the shoreline displacement rates occurred in the last 20 years using the DSAS tool of ArcGIS (Theiler et al., 2009, 2019). The multitemporal shoreline position was reconstructed using satellite images available on the Google Earth platform. According to Pantusa et al. (2022), the calculated End Point Rate (EPR) values defined the quantitative limits for the recent shoreline trends as follows:

- progradation: EPR ≥ 0.5 m a^{-1};
- equilibrium -0.5 m a^{-1} $<$EPR$<$ 0.5 m a^{-1};
- retreat: EPR: ≤ 0.5 m a^{-1}).

We coupled these data with the quantitative assessment of recent positive (e.g., uplift) or negative (e.g., subsidence) vertical ground movements (VGM) of the selected coastal plain using data from 2016 to 2022 available on the European Ground Motion Service (https://egms.land.copernicus.eu/).

This allowed us to produce the **Recent Trends Index** (RTI) which classifies the coastal trend as follows:

- Shoreline Retreat
- Shoreline Equilibrium
- Shoreline Progradation coupled with uplift
- Shoreline Progradation coupled with subsidence or tectonic stability

To define the **expected morpho-evolutive trend,** we used RSLR (relative sea level rise) rates scenarios for the next decades (up to 2100) on the basis of the projections provided in the last IPCC Assessment Report (AR6, 2023) under different scenarios (i.e., SSP2-4.5, SSP3-7, SSP5-8.5). The expected sea-level rates were corrected according to the local coastal subsidence rates estimated for each investigated plain using the Copernicus data (see above). The so obtained rates were used to further classify the expected behaviour of the coastal plains to the future sea-level rise based on their past response to different rates of sea-level changes.

In detail, we defined the Millennial trend index (HTI) by comparing the expected RSL rates with the evaluated Holocene rates for each plain. The Holocene rates were grouped in three ranges depending on the related coastal morphodynamic response (retreat, equilibrium, progradation), as follows:

- Retreat phase: Sea-level rise rates are so high that sedimentary processes cannot balance them. Consequently, shorelines move back and the coastal systems are dominated by submersion processes.
- Equilibrium phase: Sea-level rise rates are balanced by sedimentary processes and the coastal systems are characterized by a general equilibrium condition.
- Progradation phase: Sea-level rise rates are so low that coastal sedimentary processes prevail. Consequently, shorelines move seaward and the coastal systems are dominated by progradation processes.

The MTI is classified as follows:

Class 1: Expected rate of RSL > range of Holocene rates of RSLR in the coastal retreat phase

Class 2: Expected rate of RSL = range of Holocene rates of RSLR in coastal retreat phase

Class 3: Expected rate of RSL = range of Holocene rates of RSLR in coastal equilibrium phase

Class 4: Expected rate of RSL ≤ range of Holocene rates of RSLR in coastal progradation phase

In the case of Class 1 and Class 2, the expected SLR rates have been compared with those belonging to the Holocene period during which a coastal retreat occurred. In the case of Class 3, the expected SLR rates have been compared with those belonging to the Holocene period during which a coastal equilibrium occurred. In the case of Class 4, the expected SLR rates have been compared with those belonging to the Holocene period during which a coastal progradation occurred.

Finally, we calculated the **Coastal Plain Sensitivity Index (CPSI)** which integrates MTI classes with the RTI conditions allowing us to classify the investigated plains according to three sensitivity levels (Figure 2):

- Very High Sensitivity, the plain is considered very prone to be inundated under the expected sea level change;
- High Sensitivity, the plain is considered prone to be inundated under the expected sea level change;
- Medium Sensitivity, the plain can persist in equilibrium conditions under the expected sea level change;

When the expected sea-level change rate, including its vertical uncertainty, falls within the uncertainty of the Holocene RSL change rate (see Figure 4), we evaluated the percentage of overlap into the retreat, equilibrium and progradation sectors, respectively.

The ratio between the portion of overlap of each morpho-evolutive trend and the total overlapping area was expressed in terms of the percentage of likelihood that such morpho-evolutive trend will occur in the next decades (Figure 3). This last calculation was performed using the OCTAVE software (https://octave.org/).

3. Results

3.1 Holocene morpho-evolutive trends

In the Valencia (#1) and Rhone (#2) plains, we observe similar RSL trends (Figure 4). Sea level rose with rates by ~10 mm a^{-1} in ~1.4 ka (9.6 to 8.2 ka BP). We then observe a sudden deceleration with a rising trend lower than ~3 mm a^{-1} between 8.2 and 7.2 ka BP. The rate further decreased with average values of 0.5 mm a^{-1} and 2.0 mm a^{-1} between 7.2 and 5.8 ka BP. RSL finally rose to the present datum with average rates by ~0.1 mm a^{-1} in both plains. The marine transgression reached its maximum inland position at ~7.3 ka BP in Valencia plain and ~7.2 ka BP in the Rhone plain. This was followed by a period of equilibrium which lasted for ~ 1.4 to 1.5 ka BP and finally, by ~5.8 ka of progradation which brought the coastline to the present position.

In the Arno plain (#3), we observe a more complex coastal behaviour (Figure 4). In fact, sea-level rose with a mean rate of ~0.05 mm a^{-1} during a period of 2.3 ka (from 12.7 to 10.4 ka BP). Then, we observe a short-lived sea level stand that lasted 0.8 ka (10.4 and 9.6 ka BP) with a rising rate of 0.02 mm a^{-1}. A strong acceleration with rates up to 10 mm a^{-1} characterized the following 1.8 ka (until 7.8 ka BP), bringing the RSL at -12.8 ±1.4 m MSL. The rate slowly decreased with an average value of 2 mm a^{-1} between 7.8 and 5.5 ka BP. Finally, RSL rose to the present datum with an average value of 0.5 mm a^{-1}. In the Arno plain, the marine transgression reached its maximum inland position at ~8.0 ka BP. This was followed by a period of equilibrium which lasted for ~ 2.3 ka (from 7.8 to 5.5 ka BP) with the formation of an extensive lagoonal system and, finally, by ~5.5 ka BP, the progradation process brought the coastline to the present position.

In Tiber plain (#4), we noted a similar decrease in RSLR rates (Figure 4) during a 1.4 ka long period (from 9.4 to 8.0 ka BP), with rates passing from 10.6 mm a^{-1} to 3.4 mm a^{-1}. Then, for ~ 2.0 ka (between 8.0 and 6.0 ka BP), the rate was stable at an average value of 2 mm a^{-1} and after that, we observed a further decrease up to 0.4 m a^{-1}, which led to the present datum. As for Arno plain (#3), in Tiber plain (#4), the marine transgression reached its maximum inland position at 8.0 ka BP. This was followed by a morphodynamic equilibrium that lasted for ~ 2.0 ka (from 8.0 to 6.0 ka BP), after then, the progradation prevailed, leading to the present coastline position.

In the Volturno (#5) and Sele (#6) plains, we observe similar behaviour (Figure 4) for a 2.5 ka long phase (12.0 to 9.5 ka BP), during which the RSL slowly rose with average values of 0.5 mm a^{-1} (#5) and 0.9 mm a^{-1} (#6). Then, in both plains, the rising rates increased for ~ 2.0 ka (9.0 to 7.0 ka BP) with average rates of 7.9 mm a^{-1} in Volturno plain (#5) and 4.6 mm a^{-1} in Sele plain (#6). After this period, we noticed a quite different trend between Volturno plain (#5) and Sele plain (#6.) In fact, the present sea level position has been reached with highly variable rates in Volturno plain (#5), while the trends slowly decreased up to 0.1 mm a^{-1} in Sele plain (#6).

In both plains, the marine transgression reached its maximum inland position between 7.0 and 6.5 ka BP. This was followed by a period of equilibrium, which lasted for ~ 1.4 to 1.5 ka BP, and finally, the progradation process brought the coastline to the present position.

3.2 Recent morpho-evolutive trends

The recent evolution of Valencia, Arno and Tiber coastal plains (#1, #3 and #4) is characterized by a general shoreline equilibrium with average EPR values ranging from -0.10 m a^{-1} to 0 (see Table 1).

The Rhone, Volturno and Sele plains (#2, #5 and #6) showed a general retreat trend with average EPR values ranging from -0.8 m a^{-1} to -0.60 m a^{-1} (see Table 1).

The shoreline displacement trends for all the examined plains are strongly variable, with the highest difference rate estimated for plain #2, where the EPR ranges from 16.70 to -9.3 m a^{-1}.

Superimposed on these shoreline trends, general coastal subsidence (e.g., negative VGM values, Figure 1, Table 1) characterises the investigated Mediterranean plains. We observe maximal values in Volturno and Sele plains (#5 and #6), with subsidence rates higher than 3 mm a^{-1}, and minimum rate in Tiber plain #4, where subsidence rates do not exceed 1 mm a^{-1}. In Rhone and Arno plains (#2 and #3), subsidence rates range between 1.5 and 1.8 mm a^{-1} and, finally, in plain #1, subsidence rates decrease to 1.22 mm a^{-1}.

The coupled analysis of VGMs and recent shoreline trends indicate that a retreat phase with rates between -0.6 and -0.8 mm a^{-1} can be driven not only by a strong subsidence trend exceeding 3 mm a^{-1} (Volturno #5 and Sele #6 plains) but also by other forcing as in the case of Rhone plain where the measured subsidence rate did not exceed 1.4 mm a^{-1}.

Table 1 – Recent trends in terms of: column 1) average VGMs rates measured between 2016 and 2022 by the European Ground Motion Service (https://egms.land.copernicus.eu/) with their uncertainty in column 2; column 3, 4, 5) mean, maximum, and minimum coastline displacement rates (expressed by the End Point Rates EPRs) between 2003 and 2022;

PLAIN	Mean EPR (m a^{-1})	Max EPR (m a^{-1})	Min EPR (m a^{-1})	InSAR VGMs (mm a^{-1})	Uncertainty VGMs (mm a^{-1})
#1 - Valencia	-0.10	2.20	-3.30	-1.22	1.40
#2 - Rhone	-0.80	16.70	-9.30	-1.46	1.74
#3 - Arno	0.01	3.96	-6.40	-1.84	1.31

#4 - Tiber	0.00	7.80	-5.90	-1.03	1.45
#5 - Volturno	-0.70	3.50	-4.00	-3.28	1.23
#6 - Sele	-0.60	0.50	-1.60	-3.53	1.59

3.3 Expected morpho-evolutive trends

Under the SSP2-4.5 scenario, our results show that in all investigated plains (plains #1- #6), the expected RSL rate value overlaps the part of the curve of RSLR rate belonging to the period in which the plains were affected by a retreat trend (Figure 5), with different likelihoods.

The Valencia (#1) and Rhone (#2) plains are considered prone to retreat with a probability of 79% and 92%, respectively. Furthermore, we estimate a phase of equilibrium with a probability of 9% only for #1 and that a progradation trend will prevail only in 13% and 8% of cases in #1 and #2, respectively (Table 2).

In the Arno plain (#3), we calculate a probability of 74% for coastal retreat, 19% for the equilibrium, and 9% for the coastal progradation, as already occurred in the last 5.5 ka during the slowdown of RSL rise (Figure 5).

We reconstructed a very similar behaviour in Tiber plain, (#4), where the coastal retreat process has a probability of 78%, an equilibrium persistency 17%, and a progradation 5% (Figure 5).

For the Volturno plain, we observe that expected SLR rate values overlap the Holocene SLR rates only where the retreating trend prevails, returning a 100% proness to retreat. Finally, only in one case (Sele plain #6), did we obtain that the expected SLR rate is higher than the past ones, overlapping the uncertainty values (grey area in Figure 5).

However, it is worth noting that the range of the expected values (black bar in Figure 5) overlaps the uncertainty of the SLR rates belonging to equilibrium and progradation phases in four out of six plains (see Table 2), with variable percentage values (5% to 19%).

The results we obtained for scenarios SSP3-7.0 and SSP5-8.5, which assume that CO2 emissions will roughly double the current levels by 2100 and 2050, respectively, allow us to suppose that the investigated plains will retreat (Figure 5), except for the Arno plain where a coastline equilibrium could persist with a probability of 11% (under the scenario SSP3-7.0) and 7% (under the scenario SSP5-8.5) (see Table 2).

Table 2 – Predicted rates of RSL rise under the three IPCC scenarios considering the ongoing VGMs indicated in Table 1

PLAIN	RSLR in 2100 SSP2- 4.5			RSLR in 2100 SSP3- 7.0			RSLR in 2100 SSP5- 8.5		
	Average mm a^{-1}	Uncertainty mm a^{-1}		Average mm a^{-1}	Uncertainty mm a^{-1}		Average mm a^{-1}	Uncertainty mm a^{-1}	
#1 - Valencia	7.22	5.19	-3.31	10.22	5.19	-4.24	12.22	6.16	-4.24
#2 - Rhone	7.46	5.29	-3.47	10.46	5.29	-4.36	12.46	6.25	-4.36
#3 - Arno	7.84	5.17	-3.27	10.84	5.17	-4.21	12.84	6.14	-4.21
#4 - Tiber	8.03	4.25	-4.25	10.03	5.21	-4.25	13.03	5.21	-4.25
#5 - Volturno	9.83	5.14	-3.23	12.83	5.14	-4.17	14.83	6.12	-4.17
#6 - Sele	10.53	4.30	-4.30	12.53	5.25	-4.30	15.53	5.25	-4.30

3.4 Predicted coastal sensitivity to sea levels expected for the year 2100

Our analysis indicated that coastal sensitivity of the Mediterranean plains under the SSP2-4.5 scenario (RSLR globally ranging between 6 and 7 mm a^{-1}) results in very high values (74%-100%), even with likelihood ranging between 13% and 5% of resilience in Valencia, Arno and Tiber plains (Table 3, Figure 5). Those plains (#1, #3, #4) also present medium coastal sensitivity with a probability of 9%, 19%, 17%, respectively (Table 3, Figure 6). Finally, under this scenario, we found that Volturno and Sele plain (5# and #6) have the highest coastal sensitivity level (Table 3, Figure 6).

Consequently, the present morphodynamic conditions of the investigated plains are expected to be modified with a probability ranging between 74% and 100% (Table 3, Figure 6). Under this scenario, future coastal response to RSLR can be comparable to the one occurred during the Holocene, resulting in a highly probable retreat of the low-lying coastal sectors.

Under the SSP3-7.0 scenario, we evaluate a high sensitivity to RSLR for all the investigated plains, except for Arno plain where 11% of medium sensitivity can be supposed. Under this scenario, the present morphodynamic equilibrium of this plain will be inverted with a probability higher than 89%, favouring the coastal retreat and the consequent submersion, with rates already estimated for the Holocene. In addition, the rates we estimate for Sele plain (#6) will exceed even the highest values defined for the Early Holocene (Table 2, Figure 5).

We obtained similar results under the SSP5-8.5 scenario when the sensitivity to RSLR of the Mediterranean plains will range from high (Valencia, Arno and Tiber plains) to very high (Rhone, Volturno and Sele plains). Also under this scenario, the sole Arno plain shows a 7% probability to be characterized by medium sensitivity (Table 3, Figure 6).

Table 3 – Table of calculate Sensitivity index for the 6 investigated plains under the 3 IPCC scenarios took into account.

	SSP2- 4.5		**SSP3- 7.0**		**SSP5- 8.5**	
PLAIN	**SENSITIVITY**	**%**	**SENSITIVITY**	**%**	**SENSITIVITY**	**%**
#1 - Valencia	Very High	-	Very High	-	Very High	-
	High	79%	High	100 %	High	100 %
	Medium	9%	Medium	-	Medium	-
	Resilient/Low	13%	Resilient/Low	-	Resilient	-
#2 - Rhone	Very High	92%	Very High	100 %	Very High	100 %
	High	-	High	-	High	-
	Medium	-	Medium	-	Medium	-
	Resilient/Low	8%	Resilient/Low	-	Resilient/Low	-
#3 - Arno	Very High	-	Very High	-	Very High	-
	High	74%	High	89%	High	93%
	Medium	19%	Medium	-	Medium	7%
	Resilient/Low	8%	Resilient/Low	11%	Resilient/Low	-
#4 - Tiber	Very High	-	Very High	-	Very High	-

	High	78%	High	100 %	High	100 %
	Medium	17%	Medium	-	Medium	-
	Resilient/Low	5%	Resilient/Low	-	Resilient/Low	-
#5 - Volturno	Very High	100 %	Very High	100 %	Very High	100 %
	High	-	High	-	High	-
	Low	-	Low	-	Low	-
	Resilient	-	Resilient	-	Resilient	-
#6 - Sele	Very High	100 %	Very High	100 %	Very High	100 %
	High	-	High	-	High	-
	Medium	-	Medium	-	Medium	-
	Resilient/Low	-	Resilient/Low	-	Resilient/Low	-

4. Discussions

The coupled analysis from long (e.g., millennial) to short (e.g., decadal) coastal evolution of six Mediterranean major coastal plains provides us new insights into the dynamic response of sedimentary coasts to sea level rise. According to the IPCC projections, GMSL is expected to rise between 0.56 m (under the scenario SSP2-4.5: 0.43 m – 0.76 m) and 0.77 m (under the scenario SSP5-8.5: 0.63 m – 1.01 m) in 2100 (relative to the baseline period 1995-2014). However, the global trend may be significantly exacerbated by the local coastal subsidence, as in the case of the Mediterranean plains (e.g., Aucelli et al., 2017; Di Paola et al., 2021). Our methodological approach improves the classical "bathtub" inundation approach, considered simplistic and not capable of capturing all the variability in coastal response to sea level rise (e.g., Lopez-Doriga and Jimenez, 2020) by providing more robust analysis of the potential coastal responses to different rates of sea-level rise.

Under the SSP2-4.5 scenario, the average RSLR values in the Mediterranean low-lying areas range from 7.2 mm a^{-1} (Valencia plain) to 10.5 mm a^{-1} (Sele plains) (see Table 2). Under this scenario, the coastal sensitivity of Mediterranean plains shows high-to-very high values (74%-100%), even if with likelihood ranging between

13% and 5% of resilience in four plains (Valencia, Rhone, Arno and Tiber plains). Valencia, Arno and Tiber plains also present medium sensitivity with a probability of 9%, 19%, and 17%. Under this scenario, Volturno and Sele plains located in the southernmost sector have a 100% very high sensitivity.

Under SSP3-7.0 and SSP5-8.5 scenarios with CO_2 emissions that roughly double from current levels by 2100 and 2050 respectively (IPCC, 2023), a high-to-very high sensitivity to RSLR is also expected for all the investigated Mediterranean plains. The single exception is the Arno plain which shows 11% (SSP3-7.0) and 7% (SSP5-8.5) of medium sensitivity. Under these scenarios, the present morphodynamic equilibrium will be modified in a retreat trend with a probability of 89% (SSP3-7.0) and 93% (SSP5-8.5).

These data have major implications for the management of the Mediterranean coasts. In fact, our results show that in all the investigated coastal plains the predicted sea-level rise will results in a shift from equilibrium to retreat trends with a probability ranging between 74% and 100%. Only under the SSP2-4.5 scenario, Valencia, Rhone, Arno, and Tiber plains present a low probability (5% - 13%) to be affected by morphodynamic variations, preserving their present coastal equilibrium. However, this probability can be increased by considering the 2022 annual Greenhouse Gas Index (AGGI) measured by the NOAA Global Monitoring Laboratory (www.globalchange.gov/indicators/annual-greenhouse-gas-index). In fact, the SSP2-4.5 scenario, according to which the GHG emissions have to remain around current levels until the middle of the century, is already overtaken by an annual CO_2 increase from 1 Jan 2022 to 1 Jan 2023 of 2.19 ± 0.08 ppm (https://gml.noaa.gov/ccgg/trends/global.html).

Under the two scenarios predicting an increase in GHG concentrations (SSP3-7.0 and SSP5-8.5), the most probable morphodynamic response evaluated for all the investigated coastal plains is a coastal retreat similar to that occurred during the early Holocene stages.

5. Conclusions

According to the IPCC AR6, global sea level rise has been unavoidable for centuries to millennia with high confidence, due to the effect of present climatic conditions in terms of deep ocean warming and ice sheet melt. The ongoing magnitude and rate of this phenomenon are strictly related to the GHG emissions and socio-economic trends. However, the confidence level of RSLR projections decreases at a regional scale, especially in a close basin interacting with the Atlantic Ocean, such as the Mediterranean (Adloff et al., 2017).

Our study plays a fundamental role for improving the evaluation of coastal morphodynamic evolution to expected SL changes, assessing the long to short-term shoreline response to a modified rate of relative sea-level rise driven by climatic and local forcing. Our statistical approach focuses on the highest exposed low-lying areas, indicating a low resilience of Mediterranean plains to future sea-level rise scenarios. In the next 80 years, the investigated plains can be considered prone to retreat with high confidence (> 74% for SSP2-4.5; >89% for SPP3-7.0; > 93% for SPP5-8.5). Only if the GHG emissions will remain around current levels until the middle of the century (SSP2-4.5), we estimate a probability between 5% and 13% of sensitivity. However, the low confidence in this scenario is further reduced by the direct impacts of climate change on agriculture, water supply and fisheries amplified by the inefficient management of water, land and marine resources largely evaluated for the Mediterranean area (Cramer et al., 2018).

The sensitivity index for low-lying areas we are proposing is a step forward in the assessment of risk conditions compared to the classical inundation scenarios, as we evaluate the likelihood of retreating by statistically analysing the geomorphological response to the already-occurred SLR.

In conclusion, our procedure is effective for planning the most-suitable coastal risk-management measures, according to the IPCC report. In the case of the investigated Mediterranean plains, these measures could lead to the relocation of coastal cities and settlements considering that the shorelines have a high probability of retreating up to their early-Holocene position.

Statements & Declarations

Competing Interests

The authors declare no conflict of interest.

Author Contributions

All authors contributed to the study conception, design, data collection and analysis. All authors wrote the first draft of the manuscript commented and approved the final version of the text manuscript.

Data availability

Data will be made available on reasonable request.

Figure

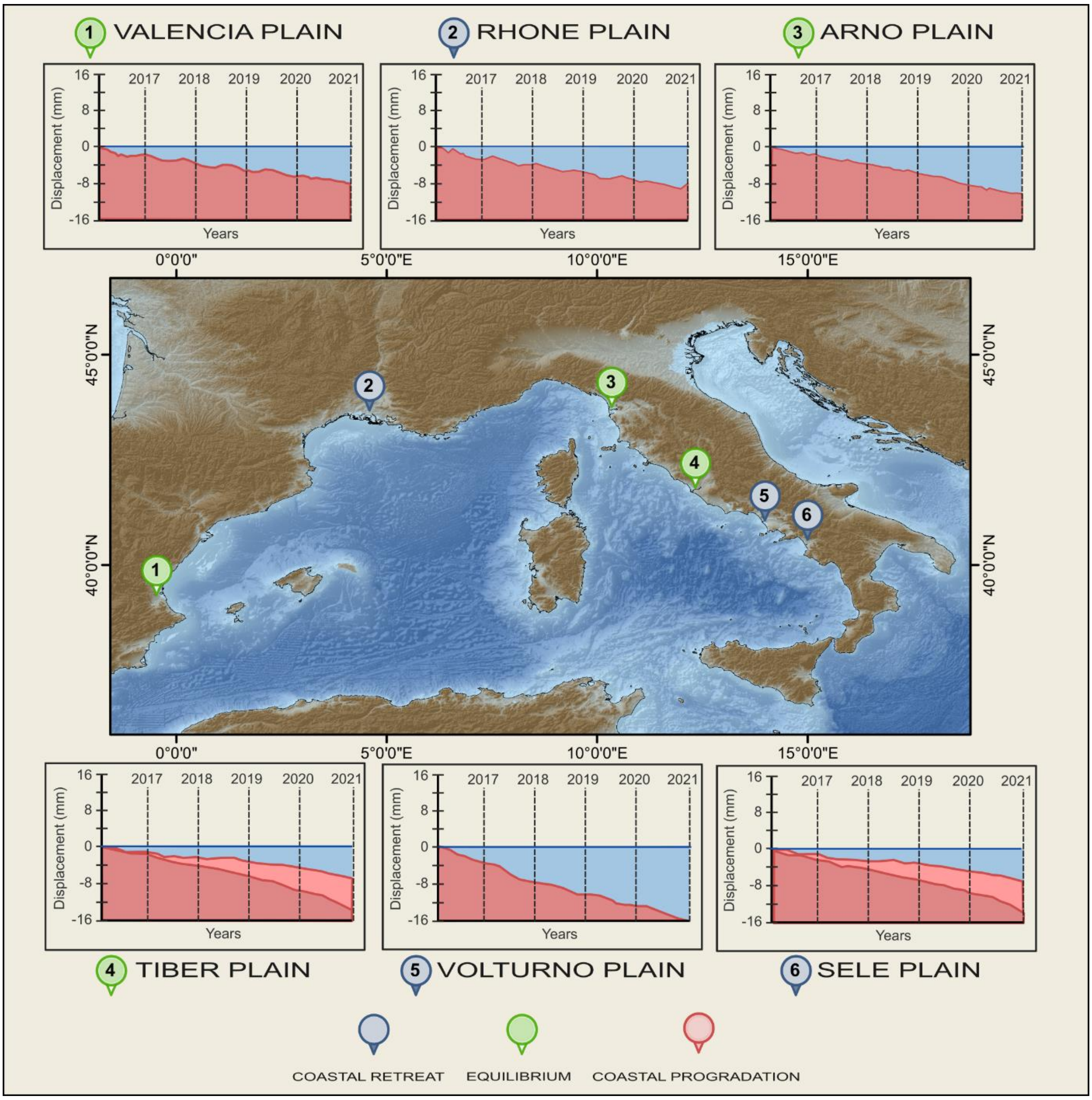

Figure 1 – Location map of the studied coastal plains with the present shoreline trend (coloured circles) and the average rates of local vertical ground movements (upper and lower boxes) measured between 2016 and 2022 by the European Ground Motion Service (https://egms.land.copernicus.eu/).

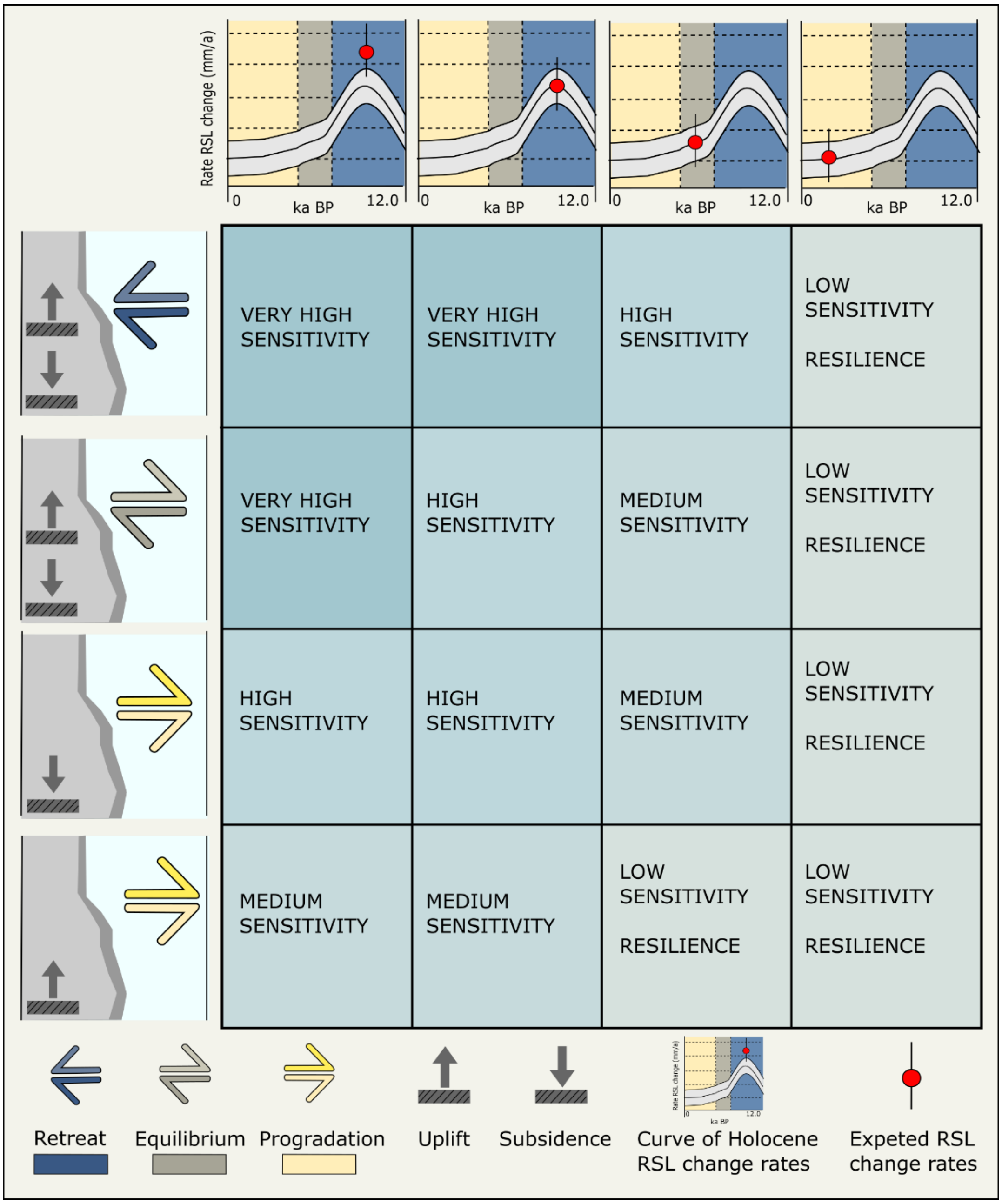

Figure 2 – Matrix of the Coastal Plain Sensitivity Index (CPSI), where the X-axis represents the possible Holocene morpho-evolutive trends compared with the future morpho-evolutive trends, according to each IPCC scenario corrected with the local subsidence, and the Y-axis represents the possible recent morpho-evolutive trends taking into account the values of the end point rates (EPR) and of the local vertical ground movements.

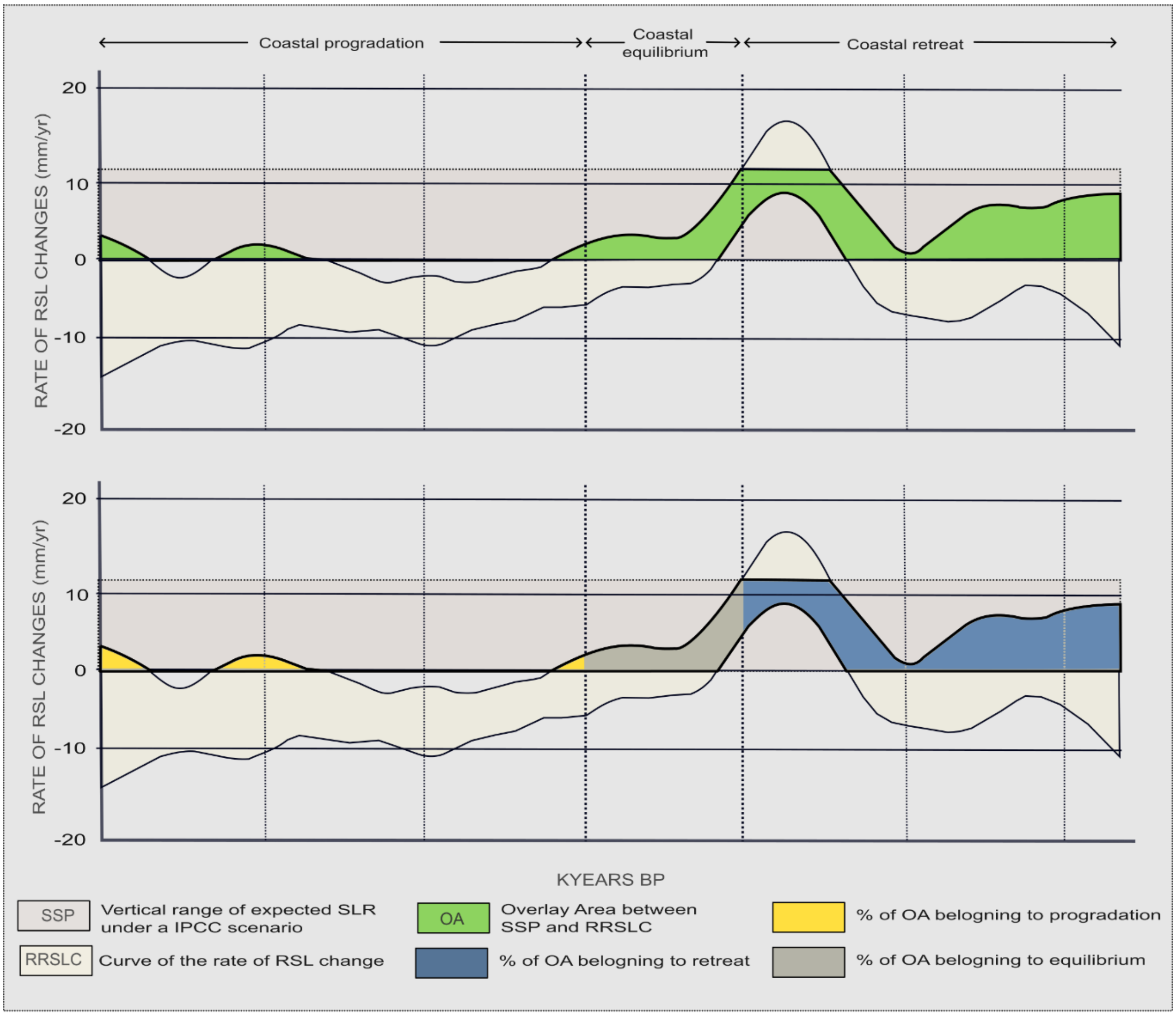

Figure 3 – Method for the evaluation of the likelihood that such morpho-evolutive trend can occur under a specific IPCC scenario, calculated as the ratio between the portion of overlap area of each morpho-evolutive trend and the total overlapping area.

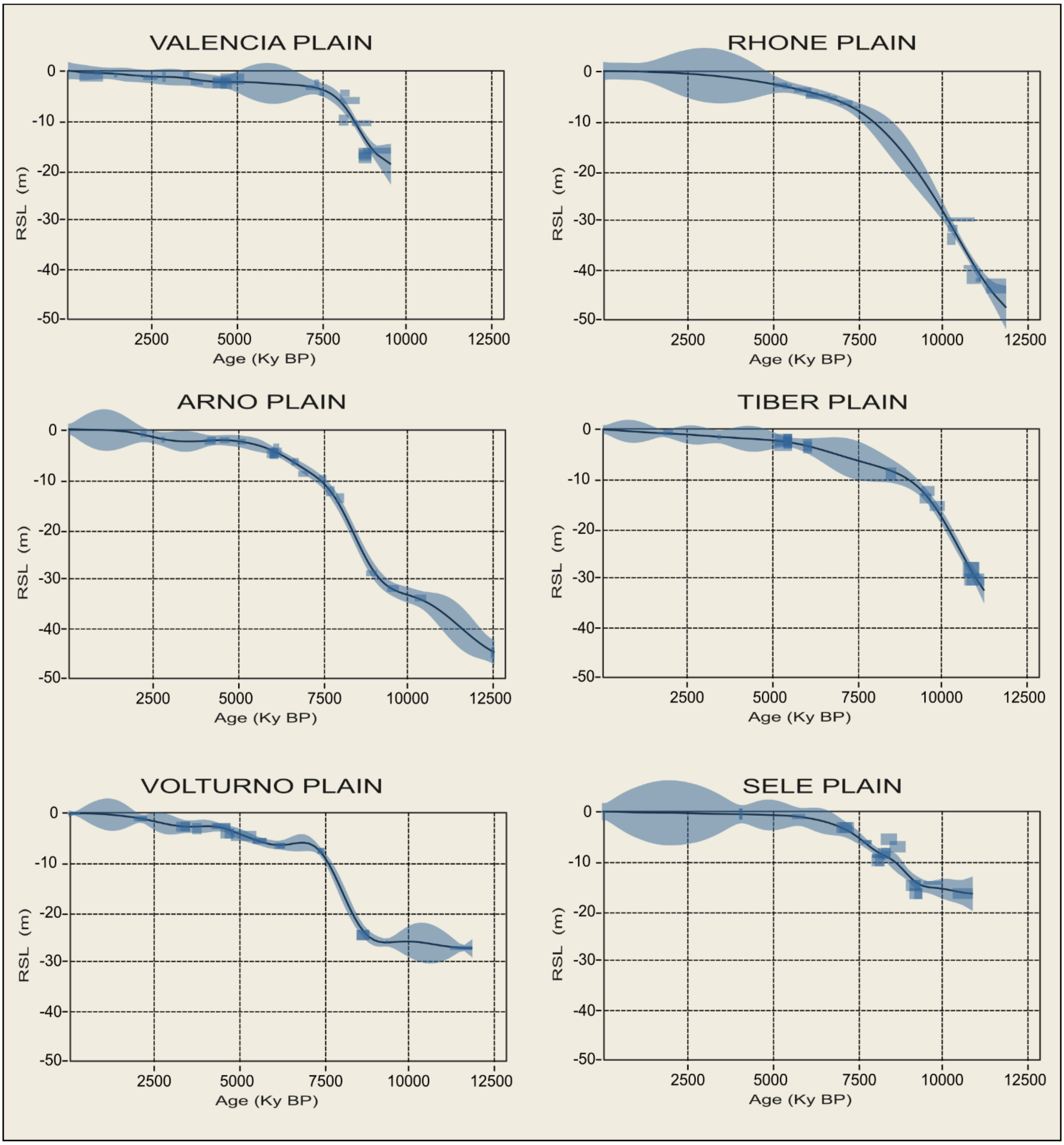

Figure 4 – RSL curves of the studied coastal plains calculated using the model Errors in Variables Integrated Gaussian Process (EIV IGP, Cahill et al., 2015) that performs Bayesian inference on historical rates of sea-level change.

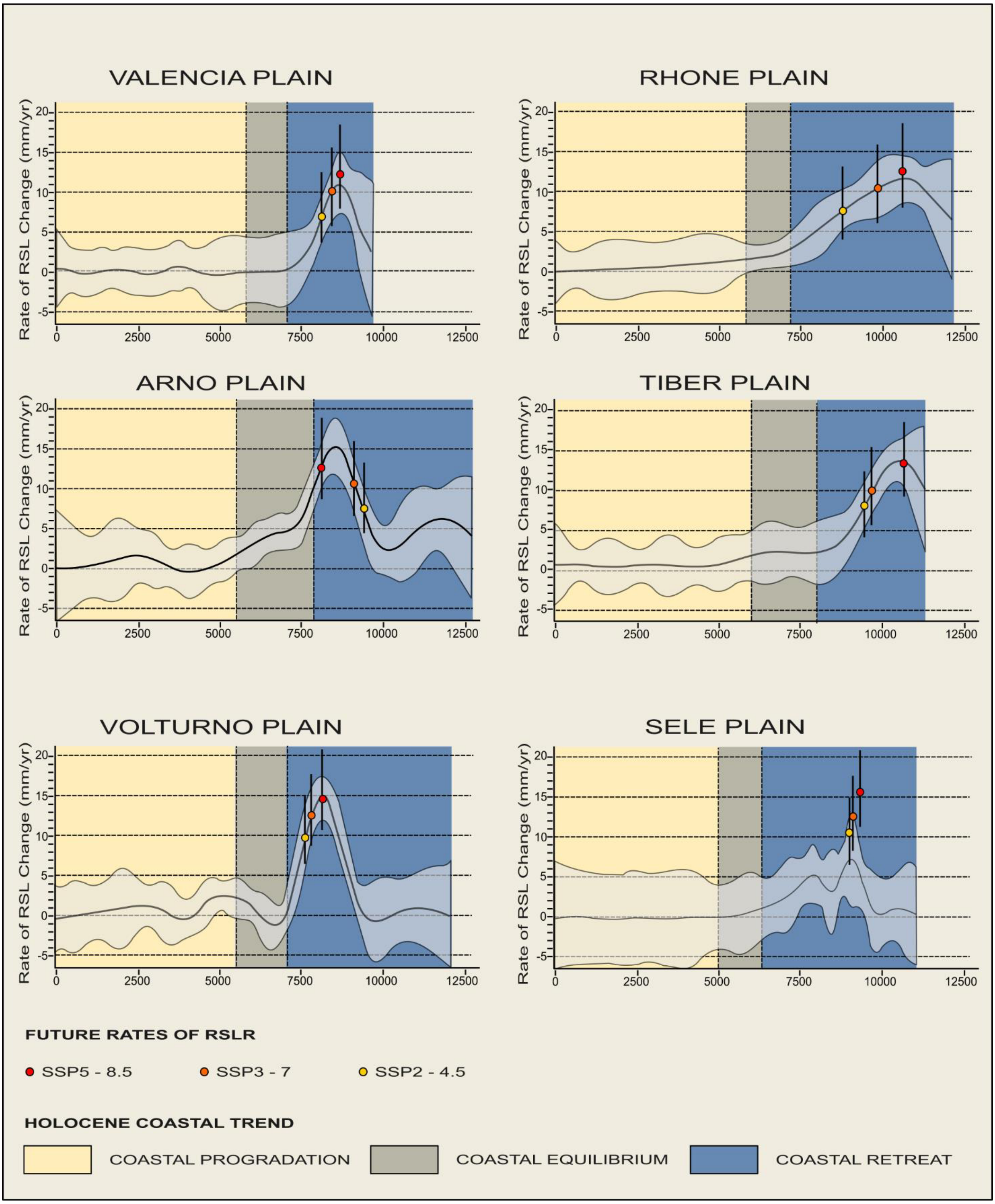

Figure 5 - Holocene curves of RSLR rates calculated using the model Errors in Variables Integrated Gaussian Process (EIV IGP, Cahill et al., 2015), with the time intervals of the different Holocene evolution phases (X-axis, blue area is retreat, grey area is equilibrium and yellow progradation) lived by the studied plains and the local RSLR rates (Y-axis) expected for the next decades (up to the year 2100) calculated taking into account different IPCC predictive scenarios (yellow circle for SSP2-4.5, orange circle for SSP3-7, red circle for SSP5-8.5) corrected with the present local coastal VGMs rates (https://egms.land.copernicus.eu/).

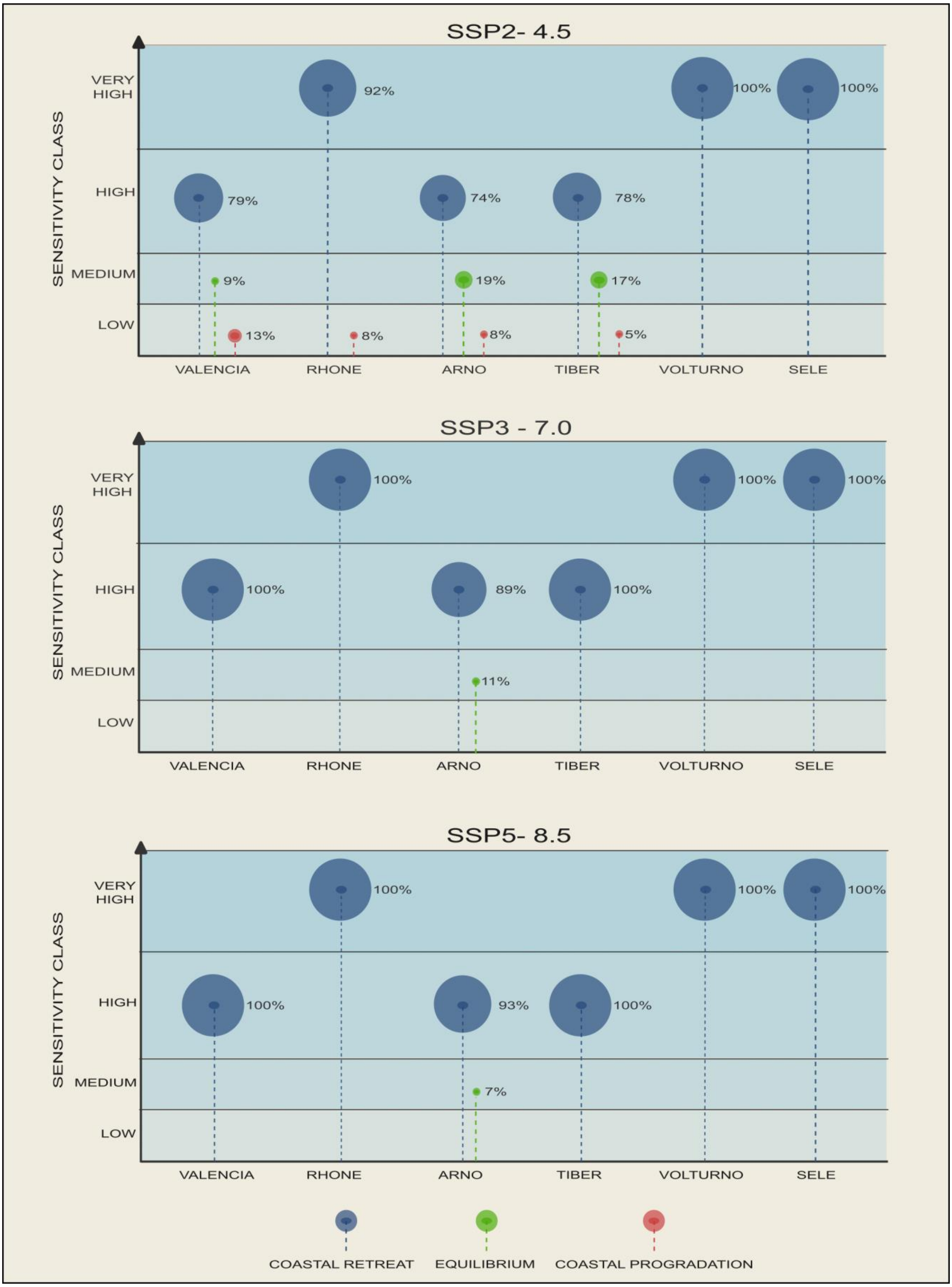

Figure 6 – Coastal sensitivity of the studied coastal plains according to the proposed methodology.

References

Adloff, F. et al. Improving sea level simulation in Mediterranean regional climate models. Clim. Dynam. 51, 1167–1178 (2017).

Anthony, E. J., Marriner, N., & Morhange, C. (2014). Human influence and the changing geomorphology of Mediterranean deltas and coasts over the last 6000 years: From progradation to destruction phase?. Earth-Science Reviews, 139, 336-361.

Antonioli, F., Anzidei, M., Amorosi, A., Presti, V. L., Mastronuzzi, G., Deiana, G., ... & Vecchio, A. (2017). Sea-level rise and potential drowning of the Italian coastal plains: Flooding risk scenarios for 2100. Quaternary Science Reviews, 158, 29-43.

Aucelli, P. P. C., Di Paola, G., Incontri, P., Rizzo, A., Vilardo, G., Benassai, G., ... & Pappone, G. (2017). Coastal inundation risk assessment due to subsidence and sea level rise in a Mediterranean alluvial plain (Volturno coastal plain–southern Italy). Estuarine, Coastal and Shelf Science, 198, 597-609

Aucelli, P.P.C.; Mattei, G.; Caporizzo, C.; Cinque; Amato, L.; Stefanile, M.; Pappone, G (2021). Multi-proxy analysis of relative sea level and paleoshoreline changes during the last 2300 years in the Campi Flegrei caldera, Southern Italy. Quaternary International, 602, pp. 110–130

Cahill, N., Kemp, A.C., Horton, B.P., Parnell, A.C., 2015. Modeling Sea-level change using errors-in-variables integrated Gaussian processes. Ann. Appl. Stat. 9 (2), 547–571. https://doi.org/10.1214/15-AOAS82

Cramer, W., Guiot, J., Fader, M., Garrabou, J., Gattuso, J. P., Iglesias, A., ... & Xoplaki, E. (2018). Climate change and interconnected risks to sustainable development in the Mediterranean. Nature Climate Change, 8(11), 972-980

Degeai, J. P., Bertoncello, F., Vacchi, M., Augustin, L., de Moya, A., Ardito, L., & Devillers, B. (2020). A new interpolation method to measure delta evolution and sediment flux: Application to the late Holocene coastal plain of the Argens River in the western Mediterranean. Marine Geology, 424, 106159.

Di Paola, G., Rizzo, A., Benassai, G., Corrado, G., Matano, F., & Aucelli, P. P. (2021). Sea-level rise impact and future scenarios of inundation risk along the coastal plains in Campania (Italy). Environmental Earth Sciences, 80(17), 608.

Di Paola, G., Rizzo, A., Benassai, G., Corrado, G., Matano, F., & Aucelli, P. P. (2021). Sea-level rise impact and future scenarios of inundation risk along the coastal plains in Campania (Italy). Environmental Earth Sciences, 80(17), 608.

FitzGerald, D. M., Fenster, M. S., Argow, B. A., & Buynevich, I. V. (2008). Coastal impacts due to sea-level rise. Annu. Rev. Earth Planet. Sci., 36(1), 601-647.

Guiot, J., & Cramer, W. (2016). Climate change: The 2015 Paris Agreement thresholds and Mediterranean basin ecosystems. Science, 354(6311), 465-468.

IPCC, 2023: Climate Change 2023: Synthesis Report. Contribution of Working Groups I, II and III to the Sixth Assessment Report of the Intergovernmental Panel on Climate Change [Core Writing Team, H. Lee and J. Romero (eds.)]. IPCC, Geneva, Switzerland, pp. 35-115, doi: 10.59327/IPCC/AR6-9789291691647.

Lionello, P., & Scarascia, L. (2018). The relation between climate change in the Mediterranean region and global warming. Regional Environmental Change, 18, 1481-1493.

López-Dóriga, U., & Jiménez, J. A. (2020). Impact of relative sea-level rise on low-lying coastal areas of Catalonia, NW Mediterranean, Spain. Water, 12(11), 3252.

Mattei, G., & Vacchi, M. (2023). The geographic variability of the millennial sea-level changes along the coasts of Italy. Alpine and Mediterranean Quaternary, 36(1), 63-74.

Mattei, G., Caporizzo, C., Corrado, G., Vacchi, M., Stocchi, P., Pappone, G., ... & Aucelli, P. P. (2022). On the influence of vertical ground movements on Late-Quaternary sea-level records. A comprehensive assessment along the mid-Tyrrhenian coast of Italy (Mediterranean Sea). Quaternary Science Reviews, 279, 107384

Melis, R. T., Depalmas, A., Di Rita, F., Montis, F., & Vacchi, M. (2017). Mid to late Holocene environmental changes along the coast of western Sardinia (Mediterranean Sea). Global and planetary change, 155, 29-41.

Nicholls, R. J., Lincke, D., Hinkel, J., Brown, S., Vafeidis, A. T., Meyssignac, B., ... & Fang, J. (2021). A global analysis of subsidence, relative sea-level change and coastal flood exposure. Nature Climate Change, 11(4), 338-342.

Pantusa, D., D'Alessandro, F., Frega, F., Francone, A., & Tomasicchio, G. R. (2022). Improvement of a coastal vulnerability index and its application along the Calabria Coastline, Italy. Scientific Reports, 12(1), 21959.

Sarkar, N., Rizzo, A., Vandelli, V., & Soldati, M. (2022). A literature review of climate-related coastal risks in the Mediterranean, a climate change hotspot. Sustainability, 14(23), 15994.

Shennan, I., Long, A.J., Horton, B.P. (Eds.), 2015. Handbook of Sea-Level Research. John Wiley and Sons, Chichester, West Sussex, UK

Snoussi, M., Ouchani, T., & Niazi, S. (2008). Vulnerability assessment of the impact of sea-level rise and flooding on the Moroccan coast: The case of the Mediterranean eastern zone. Estuarine, Coastal and Shelf Science, 77(2), 206-213.

Vacchi, M., Marriner, N., Morhange, C., Spada, G., Fontana, A., Rovere, A., 2016. Multiproxy assessment of Holocene relative sea-level changes in the western Mediterranean: Sea-level variability and improvements in the definition of the isostatic signal. Earth-Science Reviews 155, 172–197. doi:10.1016/j.earscirev.2016.02.002

Vacchi, M., Joyse, K. M., Kopp, R. E., Marriner, N., Kaniewski, D., & Rovere, A. (2021). Climate pacing of millennial sea-level change variability in the central and western Mediterranean. Nature communications, 12(1), 4013.

Vandelli, V., Sarkar, N., Micallef, A. S., Soldati, M., & Rizzo, A. (2023). Coastal inundation scenarios in the north-eastern sector of the Island of Gozo (Malta, Mediterranean Sea) as a response to sea level rise. Journal of Maps, 19(1), 2145918.

Vött, A. (2007). Relative sea level changes and regional tectonic evolution of seven coastal areas in NW Greece since the mid-Holocene. Quaternary Science Reviews, 26(7-8), 894-919.